INTERNATIONAL JOURNAL FOR NUMERICAL METHODS IN FLUIDS
Int. J. Numer. Meth. Fluids 2004; **44**:1337–1354 (DOI: 10.1002/fld.696)

Single-degree of freedom Hermite collocation for multiphase flow and transport in porous media

Francesco Fedele[1], Melissa McKay[1], George F. Pinder[1,*,†] and Joseph F. Guarnaccia[2]

[1]*College of Engineering and Mathematics, The University of Vermont, 213 Votey Building, Burlington, VT 05405-0156, U.S.A.*
[2]*Ciba Specialty Chemicals Corp., P.O. Box 71, Toms River, NJ 08754, U.S.A.*

SUMMARY

The classical collocation method using Hermite polynomials is computationally expensive as the dimensionality of the problem increases. Because of the use of a C^1-continuous basis, the method generates two, four and eight unknowns per node for one, two and three-dimensional problems, respectively. In this paper we propose a numerical strategy to reduce the nodal unknowns to a single degree of freedom at each node. The reduction of the unknowns is due to the use of Lagrangian polynomials to approximate the first-order derivatives over the minimal compact stencil surrounding each node. For the solvability of the problem the reduction of the number of collocation equations is done by a nodal weighting strategy. We have applied the proposed approach to enhance the efficiency of a collocation-based multiphase flow and transport simulator. Benchmark cases illustrate the higher performance of the new methodology when compared to classical Hermite collocation. Copyright © 2004 John Wiley & Sons, Ltd.

KEY WORDS: single-degree-of-freedom; Hermite collocation; Lagrangian polynomials; transport equation; NAPL; multiphase flow

1. INTRODUCTION

The classical collocation approach to the solution of differential equations has been known since at least 1937 [1]. However, it was largely through work conducted in the early 1970s (see for example References [2–6]) that the method was popularized for the solution of second-order partial-differential equations. While it was evident that the inherent simplicity

*Correspondence to: G. F. Pinder, College of Engineering and Mathematics, The University of Vermont, 213 Votey Building, Burlington, Vermont 05405-0156, U.S.A.
†E-mail: pinder@emba.uvm.edu

Contract/grant sponsor: VT EPSCoR
Contract/grant sponsor: EPS; contract grant/number: 0236976
Contract/grant sponsor: Ciba Specialty Chemicals Inc.

Received 17 July 2003
Revised 24 November 2003

of the approach held promise as a computationally efficient algorithm, the popularity of the method was limited, largely by the necessity of using C^1 continuous functions as a basis.

Recently there has been renewed interest in the collocation approach. Bialecky *et al.* [7] formulated a collocation approach for linear parabolic problems on rectangles and Li *et al.* [8] studied the problem of transverse vibrations of a clamped square plate. Elliptic boundary value problems [9], Schrodinger wave equation problems [10] and biharmonic problems [11], as well as techniques to efficiently solve the resulting approximating equations have also been studied by this group of researchers [12]. For more references about collocation methods see References [13–24].

In Wu and Pinder [26] a new numerical approach that builds upon the classical collocation approach was introduced. The method provides enhanced efficiency through a reduction in the number of degrees of freedom from two in one dimension, four in two dimensions and eight in three dimensions to one in any number of dimensions. In this current paper we extend this earlier work to consider several open theoretical questions and we also apply the method to two example problems.

In the first part of the paper we present the theoretical formulation of the new numerical methodology for the one-dimensional case. A Fourier-based analysis gives the order of convergence of the error of the derived numerical scheme. In the second part of the paper we present the application of the proposed technique to the dissolution of residual saturations of non-aqueous phase fluids in flowing groundwater.

2. THEORETICAL FORMULATION

Let us consider a general linear differential operator $\mathscr{L}$ and a boundary operator $\mathscr{B}$ which can be of Neumann, Dirichlet or Robin type. In the N dimensional bounded domain $\Omega \subset \Re^N$, the following boundary value problem is considered

$$\begin{aligned} \mathscr{L}u &= f \\ \mathscr{B}u &= g \end{aligned} \tag{1}$$

where $f, g : \Re^N \to \Re$ are given functions. Hereafter, we assume that the solution u of (1) is regular enough and as many times differentiable as we need, i.e. $u \in C^\infty$.

To present the key ingredients of the proposed method we initially consider the one-dimensional case $N = 1$ for clarity in presentation, but we consider higher dimensions in the application. On the domain $\Omega = [0, L]$, let $\Delta x = L/N_x$ be the space step for discretization, where N_x is the number of subintervals. We now define a uniform mesh $\Omega_x = \{x_j, 0 \leqslant j \leqslant N_x\}$ where $x_j = j\Delta x$.

2.1. *LOcalized COllocation Method (LOCOM)*

Let us refer to the minimum compact stencil of the generic node j, $\Omega_j \equiv [x_{j-1}, x_{j+1}]$. As indicated in Figure 1, the stencil embeds a two-subinterval element neighbourhood and has a size of $2\Delta x$, that is

$$\Omega_j = \Omega_{j,L} \cup \Omega_{j,R} \tag{2}$$

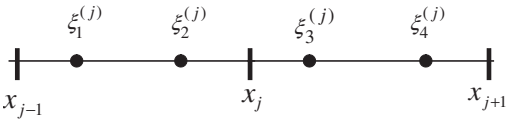

Figure 1. Template for LOCOM scheme.

where $\Omega_{j,L} \equiv [x_{j-1}, x_j]$, $\Omega_{j,R} \equiv [x_j, x_{j+1}]$ are, respectively, the left and right interval with respect to the node j.

In each stencil we have four collocation points which are located at the abscissae $\xi_k^{(j)}$ with $k = 1, 2, 3, 4$ (two collocation points for each subinterval). The Hermite approximation $\hat{u}_{\mathrm{H}}$ is the following:

$$\hat{u}_{\mathrm{H}}\left(x; \{u_q\}, \left\{ \left.\frac{\mathrm{d}u}{\mathrm{d}x}\right|_{x_q} \right\}\right) = \begin{cases} H_{0,j-1}(x)u_{j-1} + H_{1,j}(x)u_j + \tilde{H}_{0,j-1}(x) \left.\dfrac{\mathrm{d}u}{\mathrm{d}x}\right|_{x_{j-1}} + \tilde{H}_{1,j}(x) \left.\dfrac{\mathrm{d}u}{\mathrm{d}x}\right|_{x_j} & x \in [x_{j-1}, x_j] \\ H_{0,j}(x)u_j + H_{1,j+1}(x)u_{j+1} + \tilde{H}_{0,j}(x) \left.\dfrac{\mathrm{d}u}{\mathrm{d}x}\right|_{x_j} + \tilde{H}_{1,j+1}(x) \left.\dfrac{\mathrm{d}u}{\mathrm{d}x}\right|_{x_{j+1}} & x \in [x_j, x_{j+1}] \end{cases} \tag{3}$$

where the generic set $\{a_q\}$ collects the elements $\{a_{j-1}, a_j, a_{j+1}\}$ with the index q spanning $j-1, j, j+1$ and $H_{0,j}$ and $\tilde{H}_{1,j}$ are the classical Hermite polynomials (for the exact mathematical formulation of the Hermite polynomials see References [23, 24]). The collocation equations are generated by imposing the vanishing of the residual $\mathscr{L}u - f$ at the collocation points. We denote these residual equations as

$$\mathscr{R}_k^{(j)}\left(\{u_q\}, \left\{ \left.\frac{\mathrm{d}u}{\mathrm{d}x}\right|_{x_q} \right\}\right) = \mathscr{L}\hat{u}_{\mathrm{H}}(\xi_k^{(j)}) - f(\xi_k^{(j)}) = 0 \tag{4}$$

From the collocation points belonging to the template identified with node j we have available $2 \times 2 = 4$ residual equations of type shown in Equation (4) and $2 \times 3 = 6$ unknowns (two for each of the three nodes in the stencil). The problem is under-determined (more unknowns than available equations).

We want to derive a single residual equation for the node x_j which depends only on the surrounding nodal values of the function for the selected stencil, i.e. u_{j-1}, u_j, u_{j+1}. By proceeding in this way we can get one equation for each node and the well-posedness of the solution is satisfied.

2.2. *Approximation of derivatives*

In the following we shall address a way to approximate the Hermite nodal derivatives in Equation (4) as a function of the nodal values u_{j-1}, u_j, u_{j+1}. Let us set

$$\left.\frac{\mathrm{d}u}{\mathrm{d}x}\right|_{x_q} \approx \left.\frac{\mathrm{d}\hat{u}_{\mathrm{L}}}{\mathrm{d}x}\right|_{x_q} + S_q \qquad q = j-1, j, j+1 \tag{5}$$

where $\hat{u}_{\mathrm{L}}$ is the Lagrangian approximation over the stencil Ω_j, i.e.

$$\hat{u}_{\mathrm{L}}(x) = \sum_{h=j-1}^{j+1} \mathfrak{L}_{h-j+2}(x) u_h$$

with $\mathfrak{L}_s(x)$, $s = 1, 2, 3$ the Lagrangian polynomials and

$$S_q = \sum_{h=j-1}^{j+1} S_{q,h}(\Delta x) u_h \tag{6}$$

are unknown coefficients to be determined and are linearly dependent upon the nodal values. In the following we shall present a consistency-based criteria which allows us to select optimal values for $S_{q,h}(\Delta x)$ so that the convergence of the proposed scheme is optimal. Note that for the consistency of Equation (5), as the space step Δx tends to zero, S_q must approach zero (i.e. in Equation (6) we need to have $S_{q,h}(\Delta x) \to 0$ as $\Delta x \to 0$). By substituting the approximations in Equation (5) for the derivatives in the four residual equations (4) one gets four new residual equations which depend upon the nodal values of the stencil centred at the node j

$$\tilde{\mathscr{R}}_k^{(j)}(\{u_q\}; \{S_q\}) = 0 \quad k = 1, 2, 3, 4 \tag{7}$$

where

$$\tilde{\mathscr{R}}_k^{(j)}(\{u_q\}; \{S_q\}) = \mathscr{R}_k^{(j)}\left(\{u_q\}, \left\{ \left.\frac{\mathrm{d}\hat{u}_{\mathrm{L}}}{\mathrm{d}x}\right|_{x_q} + S_q \right\}\right) = 0$$

2.3. *Reduction of the residual equations*

For each node we have four residual equations and one unknown, therefore the problem is overdetermined (more equations available than unknowns). To make it solvable we consider the following averaging strategy. Within each template Ω_i we define the weighting factors for the left and right intervals as $w_{\mathrm{L}}, w_{\mathrm{R}}$ with $w_{\mathrm{L}} + w_{\mathrm{R}} = 1$. Since there are potentially four collocated residual equations of the type described in Equation (7), we derive an average collocation equation for the node j as

$$\mathbf{R}_j(\{u_q\}; \{S_q\}) = w_{\mathrm{L}} \frac{\tilde{\mathscr{R}}_1^{(j)} + \tilde{\mathscr{R}}_2^{(j)}}{2} + w_{\mathrm{R}} \frac{\tilde{\mathscr{R}}_3^{(j)} + \tilde{\mathscr{R}}_4^{(j)}}{2} = 0 \tag{8}$$

The problem now is well posed because, for each nodal unknown, we can have an averaged collocation equation. Let us specify that Equation $\mathbf{R}_j$ defines an approximation $\hat{\mathscr{L}}u$ for the operator $\mathscr{L}u$ at the jth node. In order to complete the formulation of the scheme, the coefficients S_{j-1}, S_j, S_{j+1} must be given as linearly dependent upon the unknown nodal values u_{j-1}, u_j, u_{j+1}. In the following we shall address a way to determine them based on a consistency analysis.

2.4. Consistency-based Hermite derivative approximations

The Hermite approximation $\hat{u}_{\mathrm{H}}(x)$ defined in Equation (3) can be split into two parts dependent, respectively, on the nodal function values and nodal derivative values as

$$\hat{u}_{\mathrm{H}}\left(x;\{u_q\},\left\{\left.\frac{\mathrm{d}u}{\mathrm{d}x}\right|_{x_q}\right\}\right)=\hat{u}_{\mathrm{H}}^{(1)}(x;\{u_q\})+\hat{u}_{\mathrm{H}}^{(2)}\left(x;\left\{\left.\frac{\mathrm{d}u}{\mathrm{d}x}\right|_{x_q}\right\}\right) \tag{9}$$

where we have split the approximating polynomial into the two components $\hat{u}_{\mathrm{H}}^{(1)}$ which is only dependent upon (u_{j-1},u_j,u_{j+1}) and $\hat{u}_{\mathrm{H}}^{(2)}$ which is only dependent on $(\mathrm{d}u/\mathrm{d}x|_{x_{j-1}},\mathrm{d}u/\mathrm{d}x|_{x_j},\mathrm{d}u/\mathrm{d}x|_{x_{j+1}})$. By means of the approximations (5), the Hermite approximation $\hat{u}_{\mathrm{H}}$ (see Equation (9)) can be expressed as the following:

$$\hat{u}_{\mathrm{H}}\left(x;\{u_q\},\left\{\left.\frac{\mathrm{d}u}{\mathrm{d}x}\right|_{x_q}\right\}\right)=\hat{u}_{\mathrm{H}}^{(1)}(x;\{u_q\})+\hat{u}_{\mathrm{H}}^{(2)}\left(x,\left\{\left.\frac{\mathrm{d}\hat{u}_{\mathrm{L}}}{\mathrm{d}x}\right|_{x_q}\right\}\right)+\hat{u}_{\mathrm{H}}^{(2)}(x;\{S_q\}) \tag{10}$$

By some algebra one can prove that the sum of the first two terms in Equation (10) gives the Lagrangian approximation $\hat{u}_{\mathrm{L}}(x)$ since the Lagrangian derivatives set $\{\mathrm{d}\hat{u}_{\mathrm{L}}/\mathrm{d}x|_{x_q}\}$ is forced to be the nodal derivatives in the Hermite approximation; now $\hat{u}_{\mathrm{H}}$ is of the form

$$\hat{u}_{\mathrm{H}}\left(x;\{u_q\},\left\{\left.\frac{\mathrm{d}u}{\mathrm{d}x}\right|_{x_q}\right\}\right)=\hat{u}_{\mathrm{L}}(x)+\hat{u}_{\mathrm{H}}^{(2)}(x;\{S_q\}) \tag{11}$$

We now define the discrete operator $\mathscr{L}\hat{u}_{\mathrm{H}}$ to be consistent, for any solution $u(x)$ in C^{∞}, if the difference between the $\mathscr{L}(u)$ and $\hat{\mathscr{L}}(u)$ vanishes as the space step approaches zero. That is,

$$\lim_{\Delta x\to 0}[\mathscr{L}(\hat{u}_{\mathrm{H}})-\mathscr{L}(u)]=0 \tag{12}$$

The order of convergence of this limit gives us the order of consistency of $\hat{\mathscr{L}}$. Because of Equation (11) the limit (12) is

$$\lim_{\Delta x\to 0}[\mathscr{L}(\hat{u}_{\mathrm{L}})-\mathscr{L}(u)+\mathscr{L}(\hat{u}_{\mathrm{H}}^{(2)}(x;\{S_q\}))]=0 \tag{13}$$

In general we can choose the set of parameters $\{S_q\}$ such that the order of convergence is the highest possible. The limit (13) tells us that we can choose the parameters $\{S_q\}$ so that the term $\mathscr{L}(\hat{u}_{\mathrm{H}}^{(2)}(x;\{S_q\}))$ can balance the residual error $\mathscr{L}(\hat{u}_{\mathrm{L}})-\mathscr{L}(u)$ due to the Lagrange approximation $\hat{u}_{\mathrm{L}}$ of the exact solution u. The numerical scheme thereby derived is a compact Hermite based collocation. Further studies are needed in order to determine the optimal choice of the parameters $\{S_q\}$ for various operators following the outline described above. In the following we shall show that the choice of $\{S_q=0\}$ gives optimal rates of convergence for the case of advection–diffusion operators.

3. THE ADVECTION–DIFFUSION EQUATION

We now restrict the operator $\mathscr{L}$ in Equation (1) to be the advection–diffusion operator defined as

$$\mathscr{L}u = \frac{\partial u}{\partial t} + c\,\frac{\partial u}{\partial x} - \mathscr{D}\,\frac{\partial^2 u}{\partial x^2} \tag{14}$$

Here, the velocity c and the diffusion coefficient $\mathscr{D}$ are assumed spatially constant. In Equation (5) we set $S_q = 0$. We choose as weighting factors, $w_{\mathrm{L}} \equiv \beta,\ w_{\mathrm{R}} \equiv (1-\beta)$ with $0 \leqslant \beta \leqslant 1$. The parameter β is of an up-winding type. By applying the procedure defined above, $\forall u \in C^{\infty}$ we get the averaged collocation equation relative to the node j as

$$\begin{aligned}&\mathbf{R}_j(u_{j-1}, u_j, u_{j+1})\\ &\quad = \hat{\mathscr{L}}_x u = a_1\,\frac{\mathrm{d}u_{j-1}}{\mathrm{d}t} + a_2\,\frac{\mathrm{d}u_j}{\mathrm{d}t} + a_3\,\frac{\mathrm{d}u_{j+1}}{\mathrm{d}t} + b_1 u_{j-1} + b_2 u_j + b_3 u_{j+1}\end{aligned} \tag{15}$$

where

$$\begin{aligned}&a_1 = \frac{4\beta - 1 + w^2}{8} \quad a_2 = \frac{3 - w^2}{4} \quad a_3 = \frac{3 - 4\beta + w^2}{8}\\ &b_1 = -\frac{c}{\Delta x}\left(\beta + \frac{1}{P_{\mathrm{e}}}\right) \quad b_2 = \frac{c}{\Delta x}\left(2\beta - 1 + \frac{2}{P_{\mathrm{e}}}\right) \quad b_3 = \frac{c}{\Delta x}\left(1 - \beta - \frac{1}{P_{\mathrm{e}}}\right)\end{aligned} \tag{16}$$

where we have defined the cell Peclet number as $P_{\mathrm{e}} = c\Delta x/\mathscr{D}$ and $\hat{\mathscr{L}}_x$ is the semi-discrete operator. The time derivatives in Equation (15) can be approximated by a finite difference treatment. On the time interval $[0, T]$, let $\Delta t = T/N_t$. At the $(n+1)$th time level, based on the mesh Ω_x, the discrete operator $\hat{\mathscr{L}}$ can be written as

$$\hat{\mathscr{L}}u = A_1 u_{j-1}^{n+1} + A_2 u_j^{n+1} + A_3 u_{j+1}^{n+1} + B_1 u_{j-1}^{n} + B_2 u_j^{n} + B_3 u_{j+1}^{n} \tag{17}$$

where

$$A_p = \frac{a_p}{\Delta t} + \gamma b_p \quad B_p = -\frac{a_p}{\Delta t} + (1-\gamma) b \quad p = 1, 2, 3 \tag{18}$$

in which γ is the location of the spatial operator $\hat{\mathscr{L}}_x$ in the time interval Δt.

When Equation (17) is written for each nodal location $x_j,\ j = 1, \ldots, N_x - 1$, one obtains $N_x - 2$ equations in N_x unknowns. The imposition of boundary conditions provides the required additional two equations. While first-type conditions are accommodated in the standard way by simply replacing the value of the unknown function at the boundary node, second type boundary conditions can be treated somewhat differently. Recall that we have yet to define an equation for the node at x_0 and at node x_{N_x}. While no equation is needed for the case of the first-type condition, in the case of a second-type condition the term $\partial\hat{u}/\partial x|_{x_0}$ is replaced prior to the approximation of the derivatives. While this is not especially interesting in a one-dimensional problem because of its simplicity, the implications for multidimensional problems

are quite important. Recalling that in a two-dimensional problem there are four degrees of freedom per node, it becomes apparent that there are two conditions imposed on each side node of the domain, and three conditions imposed at corner nodes. This is unique to the collocation approach.

3.1. The optimal scheme

In the formulation of the numerical scheme described by Equation (17) we have defined three parameters which are, respectively, the time-weighting factor γ, the collocation point location w and the up-wind factor β. In the following we shall choose $\gamma = \frac{1}{2}$ to get a Crank–Nicolson scheme in time. We shall derive expressions for the coefficients w and β which gives an optimal rate of convergence of the error $\mathscr{E}(\Delta x, \Delta t) = u(x,t) - \hat{u}(x,t)$ with $u \in C^\infty$ the exact analytical solution and $\hat{u}$ its numerical approximation. The analytical solution u satisfies the following initial boundary value problem

$$\begin{gathered} \mathscr{L}u = 0 \\ u(x,0) = u_0(x), \quad u_0 \in C^\infty \end{gathered} \tag{19}$$

and

$$u(x,t) = \sum_{k=-\infty}^{\infty} U_k, \quad U_k = v_k \mathrm{e}^{-\mathscr{D}\omega_k^2 t} \mathrm{e}^{\mathrm{i}\omega_k(x-ct)} \tag{20}$$

where U_k is the generic harmonic, $\omega_k \equiv \frac{2\pi}{L}k$ where L is the length of the domain, and the set of coefficients $\{v_k\}_{k\in Z}$ is the set of Fourier coefficients of the function $u_0(x)$. The approximating function $\hat{u}$ satisfies the corresponding discrete problem:

$$\begin{gathered} \hat{\mathscr{L}}\hat{u} = 0 \\ \hat{u}(x = x_j, 0) = u_0(x = x_j) \end{gathered} \tag{21}$$

An exact analytical expression for the approximant $\hat{u}$ can be derived since the problem here considered is one dimensional and the velocity c and the diffusion coefficient $\mathscr{D}$ are assumed spatially constant.

Let $x = x_j$ and $t = t_n$ be fixed. By imposing the requirement that $\hat{\mathscr{L}}\hat{u} = 0$ at the nodes, the following difference equation is obtained:

$$A_1\hat{u}_{j-1}^{n+1} + A_2\hat{u}_j^{n+1} + A_3\hat{u}_{j+1}^{n+1} + B_1\hat{u}_{j-1}^{n} + B_2\hat{u}_j^{n} + B_3\hat{u}_{j+1}^{n} = 0 \tag{22}$$

The general solution of this difference equation is

$$\hat{u}(x_j, t_n) = \hat{u}_j^n = \sum_{k=-\infty}^{\infty} \hat{U}_k \quad \hat{U}_k = h_k \exp(\mathrm{i}\omega_k x_j)(\rho_k)^n \tag{23}$$

where $\hat{U}_k$ is the generic harmonic and

$$\rho_k = -\frac{B_3\mathrm{e}^{\mathrm{i}\omega_k} + B_2 + B_1\mathrm{e}^{-\mathrm{i}\omega_k}}{A_3\mathrm{e}^{\mathrm{i}\omega_k} + A_2 + A_1\mathrm{e}^{-\mathrm{i}\omega_k}} \tag{24}$$

After application of the initial condition for the problems defined in Equations (19) and (21) we can easily obtain $\{h_k\}_{k=-\infty}^{\infty} = \{v_k\}_{k=-\infty}^{\infty}$. In general the coefficients ρ_k in Equation (24) do depend upon the Courant number defined as

$$C_{\mathrm{ou}} = \frac{c\Delta t}{\Delta x}$$

For stability of the numerical scheme, from Equation (23), numerical investigation yields that for every frequency $\omega_k \to |\rho| \leqslant 1$ (see Equation (24)) if and only if $\beta \geqslant \frac{1}{2}$, whatever the value of P_{e} and C_{ou}. The method is also stable for all collocation point locations, that is for all $w \in [0, 1]$.

The stability constraint on β is understood more clearly when one observes that β controls an up-winding phenomenon. As would be expected, when the equivalent of down-stream weighting is used, the scheme is not stable.

To derive the rate of convergence of the error $\mathscr{E}(\Delta x, \Delta t)$, we consider the limit of the difference between the analytical solution and the approximate solution as $\Delta x \to 0$ and $\Delta t \to 0$. For fixed (x, t), $\Delta x \to 0, \Delta t \to 0$ is equivalent to letting $j \to \infty$, and $n \to \infty$. By using Equations (20) and (23) one obtains for the error $\mathscr{E}(\Delta x, \Delta t)$ the representation that follows:

$$\mathscr{E}(\Delta x, \Delta t) = \sum_{k=-\infty}^{\infty} (U_k - \hat{U}_k) = \sum_{k=-\infty}^{\infty} U_k(1 - \mu_k) \tag{25}$$

where

$$\mu_k = \frac{(\rho_k)^n}{\mathrm{e}^{-\mathscr{D}\omega_k^2 t}\mathrm{e}^{-\mathrm{i}\omega_k c t}} \tag{26}$$

depends upon Δx and Δt. When (x, t) is fixed, the McLauren expansion for μ_k has the following form:

$$\mu_k = 1 + t\mathrm{i}\omega_k^3\chi_3 - t\omega_k^4\chi_4 + t\mathrm{i}\omega_k^5\chi_5 + o(\Delta t^3 + \Delta x^4) \tag{27}$$

where the coefficients χ_3, χ_4, and χ_5 depend only upon $\mathscr{D}, c, \Delta x, \Delta t, w$, and γ. Thus the error $\mathscr{E}$ (see Equation (25)) can be simplified as

$$\mathscr{E}(\Delta x, \Delta t) = \chi_3 t \frac{\partial^3 u}{\partial x^3} + \chi_4 t \frac{\partial^4 u}{\partial x^4} + \chi_5 t \frac{\partial^5 u}{\partial x^5} + o(\Delta x^4 + \Delta t^3) \tag{28}$$

because of the uniform convergence of both the Fourier series of $u_0(x)$ and all of its derivatives of every order (since $u_0(x)$ is assumed C^∞). The coefficients χ_3, χ_4, and χ_5 are bounded for finite values of $\mathscr{D}, c, \Delta x, \Delta t, w$. Therefore, when both Δx and Δt approach zero the error terms vanish.

For the case of non-zero diffusion the dominant coefficients are the following:

$$\begin{aligned}
\chi_3 &= \frac{1}{12} c^3 \Delta t^2 + \frac{1 - 2\beta}{2} \mathscr{D}\Delta x + \frac{1}{24} c\Delta x^2(1 - 3w^2) \\
\chi_4 &= -\frac{1}{4} \mathscr{D} c^2 \Delta t^2 - \frac{1}{24} \mathscr{D}\Delta x^2[5 + 24(-1 + \beta)\beta - 3w^2] \\
&\quad + \frac{1}{16} c\Delta x^3(-1 + w^2)(1 - 2\beta)
\end{aligned} \tag{29}$$

and the convergence rate depends upon the values of β and w. For any values of β and w, the rate of convergence with respect to Δt is quadratic as we have expected by choosing $\gamma = \frac{1}{2}$. The order of convergence with respect to Δx depends upon the choice of collocation points and the magnitude of the upwinding parameter β. In particular, if one selects $\beta > \frac{1}{2}$, the order of convergence is $O(\Delta x + \Delta t^2)$ irrespective of the location of the collocation points. The reason for this is the fact that under these circumstances the coefficient of Δx in the definition of χ_3 is always non-zero. On the other hand, if $\beta = \frac{1}{2}$, which corresponds to no upstream weighting, the coefficients χ_3 and χ_4 reduce to the expressions

$$\begin{aligned} \chi_3 &= \tfrac{1}{2}\, c^3 \Delta t^2 + \tfrac{1}{24}\, c \Delta x^2 (1 - 3w^2) \\ \chi_4 &= -\tfrac{1}{4}\, \mathscr{D} c^2 \Delta t^2 + \tfrac{1}{24}\, \mathscr{D} \Delta x^2 (1 + 3w^2) \end{aligned} \tag{30}$$

and the order of convergence is $O(\Delta x^2 + \Delta t^2)$ whatever the choice of the collocation points. Finally we have

$$(\mathscr{D} \neq 0) \quad \mathscr{E}(x,t) \approx \begin{cases} O(\Delta x^2 + \Delta t^2) & \text{if } \beta = \frac{1}{2} \ \forall w \in [0,1] \\ O(\Delta x + \Delta t^2) & \text{if } \beta \neq \frac{1}{2} \ \forall w \in [0,1] \end{cases} \tag{31}$$

For pure advection problems ($\mathscr{D} = 0$), the expressions of the dominant coefficients in $\mathscr{E}$ are the following

$$\begin{aligned} \chi_3 &= \frac{1}{12}\, c^3 \Delta t^2 + \frac{1 - 3w^2}{24} c \Delta x^2 \\ \chi_4 &= -\frac{(-1 + w^2)(-1 + 2\beta)}{16} c \Delta x^3 \\ \chi_5 &= \frac{1}{80}\, c^5 \Delta t^4 - \frac{-1 + 3w^2}{96} c^3 \Delta x^2 \Delta t^2 + \frac{\mathscr{A}}{960} c \Delta x^4 \\ \mathscr{A} &= 23 - 120\beta + 120\beta^2 - 30(1 - 2\beta)^2 w^2 + 15w^4 \end{aligned} \tag{32}$$

If one chooses non-Gaussian collocation points, i.e. $w^2 \neq \frac{1}{3}$, we can impose the vanishing χ_3 term by choosing

$$w^2 = \frac{1 + 2C_{\text{ou}}^2}{3}$$

getting $O(\Delta x^3 + \Delta t^4)$ with up-winding ($\beta > \frac{1}{2}$) and $O(\Delta x^4 + \Delta t^4)$ for $\beta = \frac{1}{2}$. Other collocation points (except Gaussian) imply an order of convergence of $O(\Delta x^2 + \Delta t^2)$.

If the Gaussian points are selected as collocation points the expressions for χ_3, χ_4, and χ_5 reduce to the form

$$\begin{aligned} \chi_3 &= \frac{1}{12}\, c^3 \Delta t^2 \\ \chi_4 &= \frac{-1 + 2\beta}{24}\, c \Delta x^3 \\ \chi_5 &= \frac{1}{80}\, c^5 \Delta t^4 + \frac{11 - 60\beta + 60\beta^2}{720}\, c \Delta x^4 \end{aligned} \tag{33}$$

and if up-winding is considered ($\beta > \frac{1}{2}$) the coefficient χ_4 is non-zero and the order of convergence is $O(\Delta x^3 + \Delta t^2)$. If one uses no up-stream weighting ($\beta = \frac{1}{2}$) χ_4 is zero and because χ_5 does not vanish, the convergence rate is $O(\Delta x^4 + \Delta t^2)$. Finally, if the collocation points are not Gaussian and we consider pure convection ($\mathscr{D} = 0$) the convergence rate is $O(\Delta x^2)$ irrespective of the value of β. When Gaussian collocation points are used one gets a convergence rate greater than that which one obtains when non-Gaussian points are employed, viz.

$$(\mathscr{D}=0) \quad \mathscr{E}(x,t) = \begin{cases} w^2 \neq \dfrac{1}{3}, \dfrac{1+2C_{\text{ou}}^2}{3} & O(\Delta x^2 + \Delta t^2) \quad \forall \beta \geqslant \frac{1}{2} \\ w^2 = \dfrac{1+2C_{\text{ou}}^2}{3} & \begin{cases} O(\Delta x^3 + \Delta t^4) & \beta > \frac{1}{2} \\ O(\Delta x^4 + \Delta t^4) & \beta = \frac{1}{2} \end{cases} \\ w^2 = \dfrac{1}{3} & \begin{cases} O(\Delta x^2 + \Delta t^2) & \beta > \frac{1}{2} \\ O(\Delta x^4 + \Delta t^2) & \beta = \frac{1}{2} \end{cases} \end{cases} \tag{34}$$

The rates of convergence obtained, are identical to the rates of a special form of the Petrov Galerkin method [25, 27, 28]. Indeed, for this special case, (see the paper of Bouloutas and Celia [27]), the equivalent coefficients as expressed in Equation (16) for Petrov Galerkin are the following:

$$\begin{gathered} (a_1)_{\text{PG}} = \frac{1}{6} + \frac{\eta}{12} + \frac{\alpha}{4} \quad (a_2)_{\text{PG}} = \frac{2}{3} - \frac{\eta}{6} \quad (a_3)_{\text{PG}} = \frac{1}{6} + \frac{\eta}{12} - \frac{\alpha}{4} \\ (b_1)_{\text{PG}} = -\frac{c}{\Delta x}\left(\frac{1+\alpha}{2} + \frac{1}{P_{\text{e}}}\right) \quad (b_2)_{\text{PG}} = \frac{c}{\Delta x}\left(\alpha + \frac{2}{P_{\text{e}}}\right) \quad (b_3)_{\text{PG}} = \frac{c}{\Delta x}\left(\frac{1-\alpha}{2} - \frac{1}{P_{\text{e}}}\right) \end{gathered} \tag{35}$$

where the parameters α and η control the distortion of the linear weighting functions by cubic or quadratic functions, respectively. Some algebra yields the relationship between the Petrov Galerkin parameters α, η and the LOCOM parameters β, w as

$$\beta = \frac{1+\alpha}{2} \quad w^2 = \frac{1+2\eta}{3}$$

4. COMPUTATIONAL EXAMPLES

4.1. Transport of a Gaussian hill

We first consider the transport of a Gaussian hill to test the order of convergence of the error of the proposed method. The very challenging case of pure convection of an initial square pulse is considered in order to compare the accuracy of the proposed methods against the widely used Eulerian based finite difference and finite element methods. The boundary value problem defined via the operator specified in Equation (14) with zero boundary conditions and initial conditions as

$$u(x,0) = u_0(x) = \exp\left[-\frac{(x-x_0)^2}{2\sigma^2}\right] \tag{36}$$

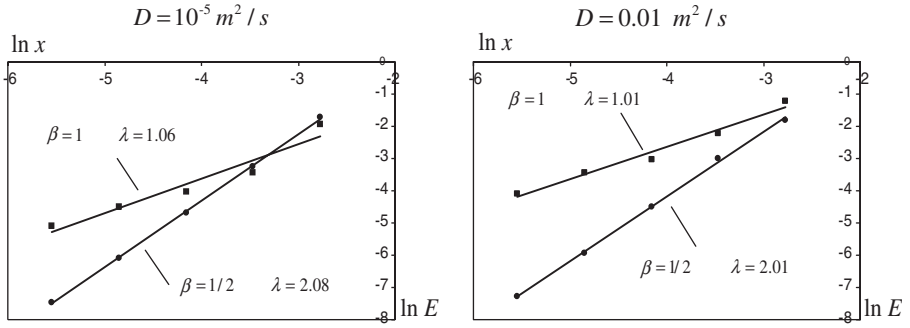

Figure 2. Convergence obtained for the case of advective-diffusive transport of a Gauss cone using $\mathscr{D} = 1.0 \times 10^{-5}\,\mathrm{m}^2/\mathrm{s}$ and $\mathscr{D} = 1.0 \times 10^{-2}\,\mathrm{m}^2/\mathrm{s}$, $c = 0.25\,\mathrm{m/s}$, $\Delta t = 1/400\,\mathrm{s}$, $\Delta x = 2^n\,\mathrm{m}$, $n = 4, 5, 6, 7, 8$, $\sigma^2 = 0.002\,\mathrm{m}^2$, and $x_0 = 0.5\,\mathrm{m}$. First-order collocation points have been used.

has a simple analytical solution which is

$$u(x,t) = \frac{\sigma}{\sqrt{\sigma^2 + 2\mathscr{D}t}} \exp\left[-\frac{(x - x_0 - ct)^2}{2(\sigma^2 + 2\mathscr{D}t)}\right] \tag{37}$$

Both the case of dominant diffusion ($\mathscr{D} \neq 0$) and pure convection ($\mathscr{D} = 0$) were examined using the sup-norm of the error as the measure. In the following we shall specify first-order and second-order collocation points for the case of $w = 0$ and $w^2 = \frac{1}{3}$, respectively. The sup-norm is given by

$$E(t) = \sup_{x \in R} |u(x,t) - \hat{u}(x,t)| \sim O(\Delta x)^{\lambda} \tag{38}$$

in which u is the exact solution, $\hat{u}$ is the numerical solution, and λ is the rate of convergence. We consider decreasing values of the spatial step as $\Delta x_k = 2^{-k}$ for different values of the integer k. In the first example we assume $\sigma^2 = 0.002\,\mathrm{m}^2$, $c = 0.25\,\mathrm{m/s}$, $x_0 = 0.5\,\mathrm{m}$, $\Delta t = 1/400\,\mathrm{s}$ and the length of the domain is $L = 1\,\mathrm{m}$. In the relationship $\Delta x_k = 2^{-k}$, $k = 4, 5, 6, 7$ and 8. The numerical error is evaluated at the 200th time step. The diffusion coefficient is given as $\mathscr{D} = 10^{-5}$ and $0.01\,\mathrm{m}^2/\mathrm{s}$. First-order collocation points are used, i.e. $w = 0$.

The plots of Figure 2 show that the order of convergence of the error depends upon the choice of β. When $\beta = 1$ the convergence rate is $O(\Delta x)$ and for $\beta = \frac{1}{2}$ the rate is $O(\Delta x^2)$. This result is consistent with the theoretical results presented in Equation (31).

Consider the case of pure advection, when Gauss points are chosen as the collocation points. Figure 3 shows the results of a calculation wherein $c = 0.25\,\mathrm{m/s}$, $\Delta t = 1/200\,\mathrm{s}$, $\Delta x = 2^n\,\mathrm{m}$, $n = 3, 4, 5, 6$, $\sigma^2 = 0.02\,\mathrm{m}^2$, $L = 5\,\mathrm{m}$ and $x_0 = 2\,\mathrm{m}$. The left-hand panel of this figure shows the rate of convergence with first-order and second-order collocation points and no up-winding. In the right-hand panel the same information is provided for the case of full up-winding. The numerical results confirm the earlier theoretical estimates which state that if Gauss points are not used as the collocation points, the pure advection case has an order of convergence of $O(\Delta x^2)$ irrespective of the up-stream weight selected. If Gauss points are used as the collocation points, $O(\Delta x^3)$ convergence is achieved with up-winding and $O(\Delta x^4)$ without up-winding. For some examples of numerical simulations the reader is referred to Reference [26].

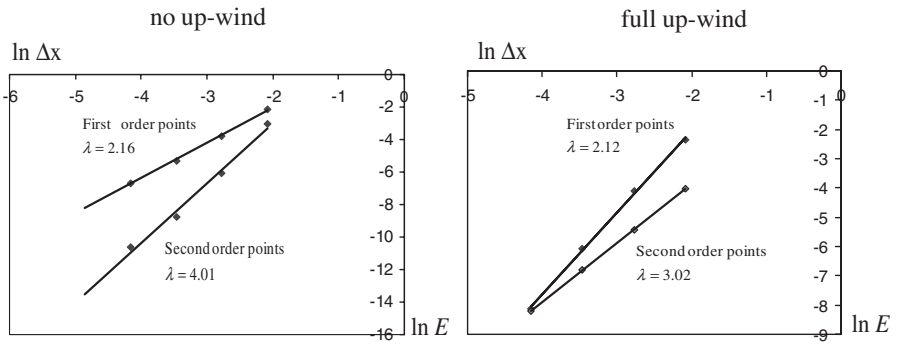

Figure 3. Convergence obtained for the case of advection of a Gauss cone using $\mathscr{D} = 0\,\mathrm{m}^2/\mathrm{s}$, $c = 0.25\,\mathrm{m/s}$, $\Delta t = 2^{-n}\,\mathrm{m}$, $n = 3, 4, 5, 6$, $\sigma^2 = 0.02\,\mathrm{m}^2$, $L = 5\,\mathrm{m}$, and $x_0 = 2\,\mathrm{m}$.

4.2. Multiphase flow and transport

The LOCOM method was implemented into an existing multiphase flow and transport code (see Reference [29]) that solves three phase and two transport equations. The general form of the equations are as follows:

Water Phase Equation

$$\varepsilon \frac{\partial S_{\mathrm{W}}}{\partial t} + \nabla \cdot q^{\mathrm{W}} = Q^{\mathrm{W}} + \frac{E_n^{\mathrm{W}} - E_{n/\mathrm{W}}^{\mathrm{G}} - E_{n/\mathrm{W}}^{\mathrm{S}}}{\rho^{\mathrm{N}r}} + \left(1 - \frac{\rho^{\mathrm{W}r}}{\rho^{\mathrm{N}r}}\right) \left\{ \frac{\varepsilon S_{\mathrm{W}} \kappa_n^{\mathrm{W}} \rho_n^{\mathrm{W}}}{\rho^{\mathrm{W}r}} - \frac{\nabla \cdot [\varepsilon S_{\mathrm{W}} D^{\mathrm{W}} \cdot \nabla \rho_n^{\mathrm{W}}]}{\rho^{\mathrm{W}}} \right\} \tag{39}$$

Gas Phase Equation

$$\varepsilon \frac{\partial S_{\mathrm{G}}}{\partial t} + \nabla \cdot q^{\mathrm{G}} = Q^{\mathrm{G}} + \frac{E_n^{\mathrm{G}} + E_{n/W}^{\mathrm{G}}}{\rho^{Nr}} + \left(1 - \frac{\rho^{\mathrm{G}r}}{\rho^{\mathrm{N}r}}\right) \left\{ \frac{\varepsilon S_{\mathrm{G}} \kappa_n^{\mathrm{G}} \rho_n^{\mathrm{G}}}{\rho^{\mathrm{G}r}} - \frac{\nabla \cdot [\varepsilon S_{\mathrm{G}} D^{\mathrm{G}} \cdot \nabla \rho_n^{\mathrm{G}}]}{\rho^{\mathrm{G}}} \right\} \tag{40}$$

NAPL Phase Equation

$$\varepsilon \frac{\partial S_{\mathrm{N}}}{\partial t} + \nabla \cdot q^{N} = Q^{N} - \frac{E_n^{\mathrm{G}} + E_n^{\mathrm{G}}}{\rho^{\mathrm{N}r}} \tag{41}$$

NAPL Contaminant Species in Water Transport

$$\varepsilon S_{\mathrm{W}} \frac{\partial \rho_n^{\mathrm{W}}}{\partial t} + \left(\frac{\rho^{\mathrm{W}}}{\rho^{\mathrm{W}r}}\right) \varepsilon S_{\mathrm{W}} \kappa_n^{\mathrm{W}} \rho_n^{\mathrm{W}} + q^{\mathrm{W}} \cdot \nabla \rho_n^{\mathrm{W}} - \nabla \left[\left(\varepsilon S_{\mathrm{W}} D^{\mathrm{W}}\right) \cdot \nabla \rho_n^{\mathrm{W}} \right] = (\tilde{\rho}_n^{\mathrm{W}} - \rho_n^{\mathrm{W}}) Q^{\mathrm{W}} + \left(1 - \frac{\rho_n^{\mathrm{W}}}{\rho^{\mathrm{N}r}}\right) [E_n^{\mathrm{W}} - E_{n/\mathrm{W}}^{\mathrm{G}} - E_{n/\mathrm{W}}^{\mathrm{S}}] \tag{42}$$

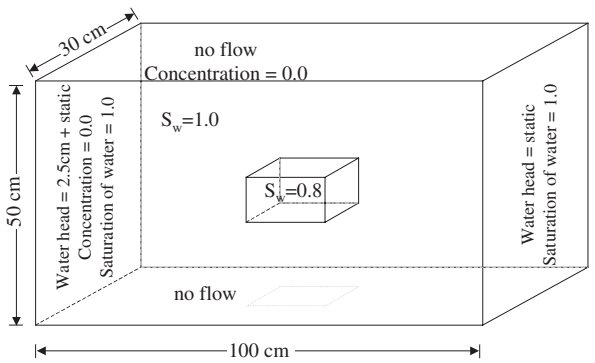

Figure 4. Three-dimensional dissolution problem set-up.

NAPL Contaminant Species in Gas Transport

$$\varepsilon S_{\mathrm{G}} \frac{\partial \rho_n^{\mathrm{G}}}{\partial t} + q^{\mathrm{G}} \cdot \nabla \rho_n^{\mathrm{G}} - \nabla[(\varepsilon S_{\mathrm{G}} D^{\mathrm{G}}) \cdot \nabla \rho_n^{\mathrm{G}}] + \frac{\varepsilon S_{\mathrm{G}} \rho^{\mathrm{G}} \kappa_n^{\mathrm{G}}}{\rho^{\mathrm{G}r}} \rho_n^{\mathrm{G}}$$
$$= (\tilde{\rho}_n^{\mathrm{G}} - \rho_n^{\mathrm{G}}) Q^{\mathrm{G}} + \left(1 - \frac{\rho_n^{\mathrm{G}}}{\rho^{\mathrm{N}r}}\right) [E_n^{\mathrm{G}} + E_{n/\mathrm{W}}^{\mathrm{G}}] \tag{43}$$

where ε is the porosity of the porous medium, S_α is the saturation of the α-phase where $\alpha = \mathrm{W}$ (water), N (NAPL), G (gas), q^α is the α-phase flux vector $[L^3/T]$, Q^α is the point source $(+)$ or sink $(-)$ of α-phase mass $[1/T]$, E_n^{W} is the mass exchange of NAPL from the NAPL phase to the water phase (dissolution) $[M/TL^3]$, $E_{n/\mathrm{W}}^{\mathrm{G}}$ is the mass exchange of NAPL contaminant species from the aqueous phase to the gas phase (evaporation) $[M/TL^3]$, $E_{n/W}^{\mathrm{S}}$ is the mass exchange of NAPL contaminant species from the aqueous phase to the solid phase (adsorption) $[M/TL^3]$, E_n^{G} is the mass exchange of NAPL from the NAPL phase to the gas phase (volatilization) $[M/TL^3]$, $\rho^{\alpha r}$ is the mass density of the pure α-phase $[M/L^3]$, κ_n^α is the decay coefficient for species i in the α-phase $[1/T]$, ρ_n^α is the mass concentration of the NAPL contaminant species in the α-phase $[M/L^3]$, D^α is the dispersion coefficient for the α-phase, a symmetric second-order tensor $[L^2/T]$ and $\tilde{\rho}_n^\alpha$ is the concentration of the injected or extracted water from source Q $[M/L^3]$.

The multiphase code used in this comparison employs a classical collocation method applied to the linearized equations [39–43]. The code was modified to employ LOCOM. No upwinding was considered and collocation equations were written at the Gauss points. The two methods were compared in terms of accuracy and computational efficiency.

4.2.1. Dissolution problem setup. The problem set-up is as seen in Figure 4. The domain of interest is a $50 \times 100 \times 30$ cm box. The box has an initial water saturation (S_{w}) of 1.0, with the exception of a $30 \times 40 \times 10$ cm box located approximately in the center of the domain, where a residual saturation of non-aqueous phase liquid (NAPL) of 0.2 ($S_{\mathrm{w}} = 0.8$) is imposed. The NAPL is considered to be at its residual saturation and is thereby an immobile phase (note that this is not a limitation of the method). A 2.5 cm water gradient is imposed from left

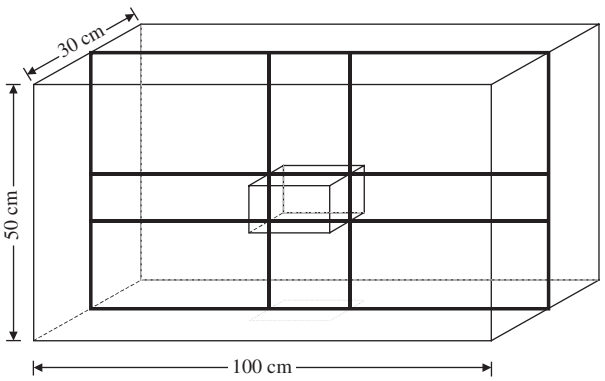

Figure 5. Representative slice taken of the domain to show the results from the sample problem.

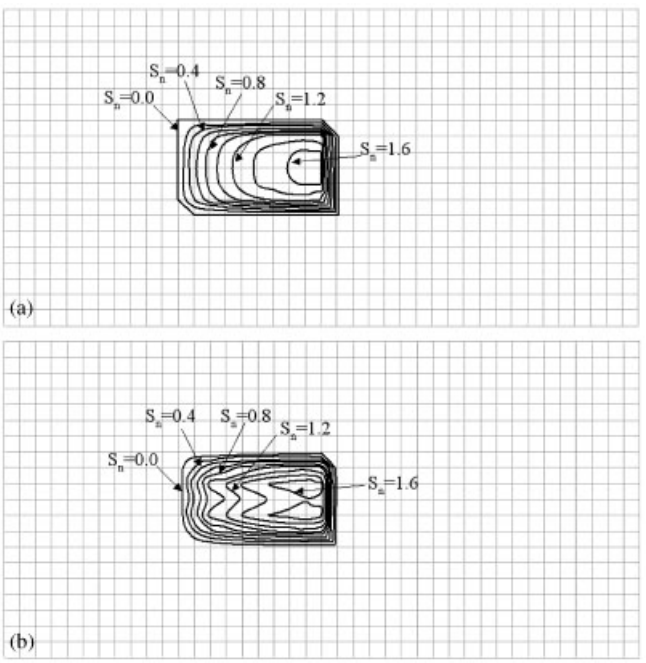

Figure 6. The results of the concentration of NAPL contaminant species in the water phase for (a) the classical collocation method and (b) LOCOM, at time = 256 000 s.

to right across the box, with no flow conditions present on the top, bottom, front and back. A Dirichlet condition of zero concentration of aqueous NAPL contaminant species is imposed on the left and top of the box, with zero-flux Neumann conditions defined elsewhere. A zero NAPL saturation condition is imposed on the left and right of the box and a zero flux of NAPL elsewhere.

The NAPL contaminant species is then allowed to dissolve into the water phase for 800 000 s. The problem was run using four different grid spacings, $\Delta x = \Delta y = \Delta z = 10, 5, 2.5$

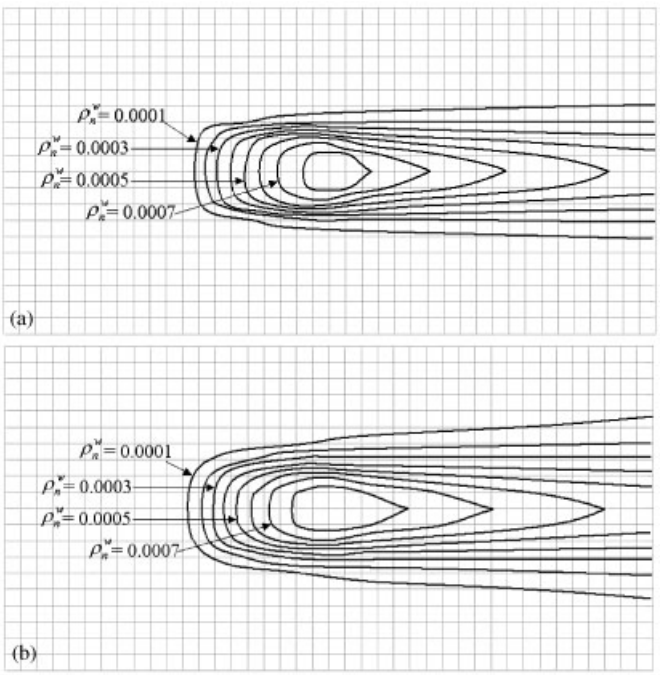

Figure 7. The results of the concentration of NAPL contaminant species in the water phase for (a) the classical collocation method and (b) LOCOM, at time = 256 000 s.

and 1.25 cm. Visual comparisons of the results for saturation of NAPL (S_n) and concentration of NAPL contaminant species in water (ρ_n^w) were then examined and the computational time was recorded. A representative slice of the domain, as shown in Figure 5, was taken to view the results.

4.2.2. Visual comparison of results. A comparison of the two methods depicting the saturation of NAPL and the concentration of NAPL contaminant species at time $t = 256\,000$ s is found in Figures 6 and 7, respectively. The saturation solutions appear to be similar in the amount of residual NAPL remaining in the domain, although the shape of the curves are slightly different. The concentration results for the two methods are very similar, though the LOCOM solution is slightly more diffused than the classical method.

4.2.3. Computational efficiency. The computational time required for a solution was determined for both methods for the four different grid spacings mentioned previously. The results can be seen in Table I.

4.2.4. Error analysis. A similar problem to that shown in Figure 6 was run in two dimensions and an error analysis was performed on the results. The classical collocation method at the smallest grid spacing was used as the 'exact' solution. The grid spacings of $\Delta x = \Delta y = \Delta z = 10, 5, 2.5$ and 1.25 cm were then analysed and the results can be seen in Figures 8 and 9.

Table I. A comparison of computation time versus the number of nodes in the system (in seconds).

Number of nodes	Hermite (s)	LOCOM (s)	Speed up
264 ($6 \times 11 \times 4$)	88.61	37.92	2.3
1617 ($11 \times 21 \times 7$)	834.03	348.06	2.4
11 193 ($21 \times 41 \times 13$)	8,823.88	2,700.33	3.3
83 025 ($41 \times 81 \times 25$)	Non convergent	22,680.69	—

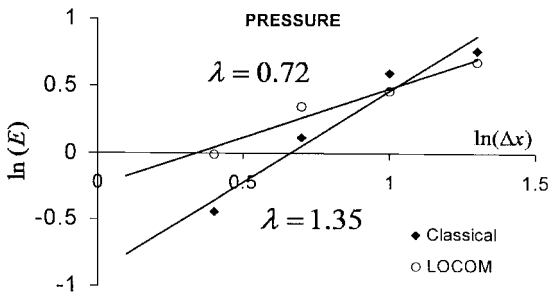

Figure 8. Rates of convergence of LOCOM and classical collocation pressure solutions.

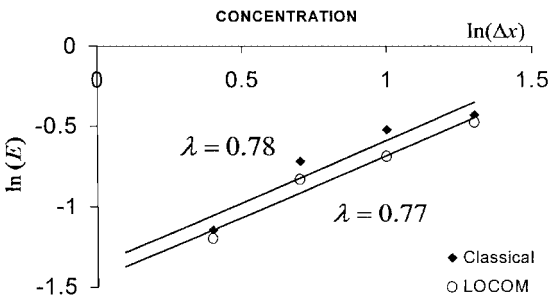

Figure 9. Rates of convergence of LOCOM and classical collocation concentration solutions.

5. CONCLUSION

We propose a new numerical technique which enhances the performance of the classical Hermite collocation method. Reduction in the degrees of freedom can be obtained while maintaining higher accuracy. The nodal derivatives which are unknowns in classical Hermite collocation are approximated as functions of the nodal values of the minimal compact stencil relative to each node. Optimal approximations for the nodal derivatives can be chosen such that the truncation error of the discretized operator has the highest order of convergence. The new numerical technique has been applied to an existing multiphase transport code based on Hermite collocation.

ACKNOWLEDGEMENTS

The authors wish to acknowledge the financial support of the Vermont Experimental Program to Stimulate Competitive Research (VT EPSCoR), EPS, grant number EPS - 0236976 and the Ciba Specialty Chemicals Inc.

REFERENCES

1. Frazer RA, Jones WP, Skan SW. Approximations to functions and to the solution of differential equations. *Aero. Res. Comm.* 1937; Report and Memorandum No. 1799 (2913); 33.
2. De Boor C, Schwartz B. Collocation at Gaussian points. *SIAM Journal on Numerical Analysis* 1973; **10**: 582–606.
3. Cavendish JC. A collocation method for elliptic and parabolic boundary value problems, using cubic splines. *Ph.D. Thesis*, University of Pittsburgh, PA, 1972.
4. Douglas J, Dupont T. *Collocation methods for parabolic equations in a single space variable Based on C^1-piecewise-polynomial spaces*, Lecture Notes in Mathematics, vol. 385. Springer: Berlin, New York, 1974:65, iv+147.
5. Finlayson BA. *The Method of Weighted Residuals and Variational Principles*. Academic Press: New York, 1972.
6. Prenter PM. *Splines and Variational Methods*. Wiley Interscience: New York, 1975.
7. Bialecky B, Fernandes RI. An orthogonal spline approximation alternating direction implicit Crank–Nicolson method for linear parabolic problems. *SIAM* 1999; **36**:1414–1434.
8. Li B, Fairweather G, Bialecky B. Discrete-time orthogonal spline collocation methods for vibration problems. *SIAM Journal on Numerical Analysis* 2002; **39**(6):2045–2065.
9. Bialecky B. Convergence analysis of orthogonal spine collocation for elliptic boundary problems. *SIAM Journal on Numerical Analysis* 1998; **35**(2):617–631.
10. Li B, Fairweather G, Bialecky B. Discrete-time orthogonal spline collocation methods for Schrodinger equations in two space variables. *SIAM Journal on Numerical Analysis* 1998; **35**(2):453–477.
11. Lou Z, Bialecky B, Fairweather G. Orthogonal spline collocation methods for biharmonic problems. *Numerische Mathematik* 1998; **80**:267–303.
12. Bialecky B, Fairweather G. Matrix decomposition algorithms in orthogonal spline collocation for separable elliptic boundary value problems. *SIAM Journal on Scientific Computing* 1995; **16**(2):330–347.
13. Bialecky B, Fernandes RI. An orthogonal spline collocation alternating direction implicit method for second-order hyperbolic problems. *IMA Journal on Numerical Analysis* 2003; **23**(4):693–718.
14. Bialecky B. Convergence analysis of orthogonal spline collocation for elliptic boundary problems. *SIAM Journal on Numerical Analysis* 1998; **35**(2):617–631.
15. Bialecky B. SuperConvergence analysis of the orthogonal spline collocation solution of Poisson's equation. *Numerical Methods for Partial Differential Equations* 1998; **15**:285–303.
16. Bialecky B, Fairweather G. Matrix decomposition algorithms in orthogonal spline collocation for separable elliptic boundary value problems. *SIAM Journal on Scientific Computing* 1995; **16**(2):330–347.
17. Bialecky B, Remington KA. Fourier matrix decomposition methods for the least squares solution of singular Neumann and periodic Hermite bicubic collocation problems. *SIAM Journal on Scientific Computing* 1995; **16**(2):431–451.
18. Frind EO, Pinder GF. A collocation finite element method for potential problems in irregular domains. *International Journal for Numerical Methods in Engineering* 1979; **14**:681–701.
19. Bentley LR, Aldama A, Pinder GF. Fourier analysis of the Eulerian–Lagrangian least squares collocation method. *International Journal for Numerical Methods in Fluids* 1990; **11**:427–444.
20. Celia MA. Collocation on deformed finite elements and alternating direction collocation methods. *Ph.D. Dissertation*, Department of Civil Engineering, Princeton University, Princeton, New Jersey, 1983.
21. Allen MB, Murphy CL. A finite-element collocation method for variably saturated flow in two space dimensions. *Water Resources Research* 1986; **22**(11):1537–1542.
22. Allen MB, Herrera I, Pinder GF. *Numerical Modeling in Science and Engineering*. Wiley: New York, 1988.
23. Lapidus L, Pinder GF. *Numerical Solution of Partial Differential Equations in Science and Engineering*. Wiley: New York, 1982.
24. Botha JF, Pinder GF. *Fundamental Concepts in the Numerical Solution of Differential Equations*. Wiley: New York, 1983.
25. Wang H, Dahle HK, Ewing RE, Espedal MS, Sharpley RC, Man S. An ELLAM scheme for advection–diffusion equations in two dimensions. *SIAM Journal on Scientific Computing* 1999; **20**(6):2160–2194.
26. Wu L, Pinder GF. Single-degree collocation method using Hermite polynomials. *Contemporary Mathematics* 2002; **295**:489–499.

27. Bouloutas ET, Celia MA. An improved cubic Petrov–Galerkin method for simulation of transient advection–diffusion processes in rectangularly decomposable domains. *Computer Methods in Applied Mechanics and Engineering* 1991; **92**:289–308.
28. Westerink JJ, Shea D. Consistent higher degree Petrov–Galerkin methods for the solution of the transient convection–diffusion equation. *International Journal for Numerical Methods in Engineering* 1989; **28**: 1077–1101.
29. McKay M, Pinder GF, Fedele F, Guarnaccia J, Wu L. Multiphase groundwater flow and transport using a new localized collocation method (LOCOM). *Computational Methods in Water Resources*, XIV, Delft, The Netherlands 2002; 241–248.
30. Pinder GF, Guaranaccia JF. A collocation based parallel algorithm to solve immiscible two phase flow in porous media. In *Computational Methods in Subsurface Hydrology*. Computational Mechanics Publications, Springer: Berlin, 1990; 205–210.
31. Pinder GF, Guarnaccia JF. *A New Two-Phase Flow and Transport Model with Interphase Mass Exchange Computational Methods in Water Resources*. Computational Mechanics Publications (Elsevier Applied Science) 1992; **2**:281–296.
32. Pinder GF, Guarnaccia JF. NAPL: Simulator Documentation. *National Risk Management Research Laboratory, U.S. Environmental Protection Agency* 1997; EPA/600/SR-97/102; 8.

